

## Competition between suppression and production of Fermi acceleration

Denis Gouvêa Ladeira<sup>1</sup> and Edson D. Leonel<sup>2</sup>

<sup>1</sup>*Campus Alto Paraopeba, Universidade Federal de São João Del-Rei, Fazenda do Cadete, CEP 36420-000, Ouro Branco, MG, Brazil*

<sup>2</sup>*Departamento de Estatística, Matemática Aplicada e Computação, Instituto de Geociências e Ciências Exatas, Universidade Estadual Paulista, Av. 24A, 1515, Bela Vista, CEP 13506-700, Rio Claro, SP, Brazil*

(Received 2 September 2009; revised manuscript received 20 January 2010; published 23 March 2010)

The behavior of the average velocity for a classical particle in the one-dimensional Fermi accelerator model under sawtooth external force is considered. For elastic collisions, it is known that the average velocity of the particle grows unlimitedly because of the discontinuities of the derivative of the moving wall's position with respect to time. However, and contrary to what was expected to be observed, the introduction of a friction force generated from a slip of a body against a rough surface leads to a *boundary* separating different regions of the phase space that yields the particle to either experience unlimited energy growth or suppression of Fermi acceleration. The Fermi acceleration is described by using scaling arguments. The formalism presented can be extended to two-dimensional time-dependent billiards as well as to higher-order mappings.

DOI: [10.1103/PhysRevE.81.036216](https://doi.org/10.1103/PhysRevE.81.036216)

PACS number(s): 05.45.Pq

Since the discovery of the cosmic rays in the last century [1] a big effort has been employed on the study and understanding of this kind of radiation. However, the physical mechanism of the acceleration process of the high-energy cosmic rays is still to be understood. The so called cut-off energy (the upper limit on the energy that cosmic ray retains) is another phenomena of recent investigation [2–5]. Moreover, it is unknown whether the cutoff occurs due to propagation effects or due to physical limitations of the acceleration process [6]. All these facts suggest that the subject deserves further investigation and therefore many models have been proposed and studied along last decades.

In 1949, Fermi [7] launched the idea that a possible mechanism was related to scattering of a cosmic particle with a time moving magnetic field. His original idea was later investigated generating many mathematical models and producing a wide class of interesting results with applicability in tokamaks [8,9], waveguide [10,11], time-dependent oscillating square wells [12,13], chaotic dynamics and phase transition [14], and many other.

One of the mathematical models [15] considers that the cosmic ray is replaced by a classical particle and that the time varying magnetic field is described by an infinitely heavy and periodically moving wall. The returning mechanism of the particle for a next collision with the moving wall is made by a fixed and rigid wall. Indeed, if the particle travels freely between the two walls and the position of the moving wall is given by  $x_w = \epsilon \cos(\omega t + \phi_0)$ , where  $\epsilon$  is the amplitude of oscillation,  $\omega$  is the frequency of oscillation, and  $\phi_0$  is an initial phase, it is known that the phase space of this model presents a mixed structure. Therefore it is observed fixed points involved by Kolmogorov-Arnold-Moser (KAM) islands, regions of nondissipative chaotic motion (chaotic seas) and invariant spanning curves (also called as invariant tori). The first chaotic region is limited by the lowest-energy spanning curve. The presence of the spanning curves limits the values of velocity and hence the energy of the particle is bounded, consequently no Fermi acceleration (FA) is observed [15,16]. The phenomenon of FA is a process in which a classical particle acquires unbounded energy from collisions with a heavy moving wall.

The mixed structure of the phase space is totally destroyed if dissipation is introduced. If the particle experiences a fractional loss of energy upon collision with the walls, the invariant spanning curves are destroyed. The elliptic fixed points turn into sinks. Depending on the control parameters, boundary crisis can be characterized via crossing of stable and unstable manifolds. For the limit of high dissipation, it is possible to observe bifurcation cascades. For the dissipative dynamics, attractors are created in the phase space. Hence FA is not observed. If one consider the motion of the moving wall to be random, the nondissipative dynamics yields in the unlimited energy growth [17]. However, the introduction of inelastic collisions is a sufficient condition to suppress FA [18–20]. Other kind of dissipation assumes that the particle is moving in the presence of a drag force such as gas. Such dissipation acts along the full trajectory of the particle and is contrary to the inelastic collisions which act only in the instant of the impact. For the case of damping force proportional to the particle's velocity, the phenomenon of FA is suppressed [21].

In this work we revisit the dynamics of a classical particle in the one-dimensional Fermi accelerator model under an external force of sawtooth type seeking to understand and describe a competition between FA and suppression of FA. The choice of such an external perturbation of sawtooth type is because the oscillating wall always furnishes energy to the particle after each collision. Thus in the absence of any dissipation, FA is feasible. The main question to be answered is: does the FA remains observed under the presence of a friction force generated from a slip of a body against a rough surface? The answer is not so simple and we will show it depends on the initial conditions as well as on the control parameters. Thus, our main goal in this paper is to investigate the consequences of dissipation due to friction in the FA process. Our results can be extendible to many other models including a wide class of two-dimensional time-dependent billiards.

Regarding the moving wall we discuss two situations: (i) the case where the wall presents stochastic motion and (ii) the case where the wall moves according a sawtooth expression. We will discuss the first situation later. Let us now

regard the second situation, where the wall moves according to the expression  $x_w(t) = (\epsilon\omega t' + \mathcal{X}_0) \bmod(2\epsilon) - \epsilon$ . The symbol  $\epsilon$  represents the amplitude of motion,  $\omega$  is the frequency of oscillation,  $t'$  is the time, and  $\mathcal{X}_0 \in [0, 2\epsilon)$  defines the initial position of the wall  $x_w(t'=0)$ . According to this expression, the moving wall oscillates between the positions  $x = -\epsilon$  and  $x = \epsilon$ . The fixed wall is at position  $x = l$ . In terms of dimensionless variables we have that  $X = x/l$  and  $V = v/(l\omega)$  furnish the position and velocity of both particle and wall. In addition  $\epsilon = \epsilon/l$  and  $t = \omega t'$  are the amplitude of oscillation of the moving wall and time. In terms of this set of variables the velocity of the wall is fixed as  $V_w = \epsilon$  and we have that  $\chi_0 = \mathcal{X}_0/l \in [0, 2\epsilon)$ .

If we take into account nondissipative dynamics, the velocity and hence the kinetic energy of the particle increases at each collision with the moving wall. Therefore, the moving wall always gives energy to the particle and such system represents a good prototype to produce FA. The velocity of the particle after each collision is given by

$$V_{n+1} = V_n + 2\epsilon = V_0 + (n+1)\epsilon, \quad n \geq 0. \quad (1)$$

On the other hand, if dissipation is introduced, the dynamics of the particle has a profound modification. In particular, the results might reveal presence or lack of FA, depending on the intensity of dissipation as well as on the amplitude of oscillation and also on the initial conditions. The dissipation we are considering occurs when a body slips on a rough surface. This kind of dissipation acts in a body throughout its entire trajectory. Thus, while the particle moves between the walls, a constant force  $F = \pm \mu mg$  acts on the particle then decreasing its energy. Here  $m$  is the particle's mass,  $g$  is the gravitational acceleration, and  $\mu$  is the kinetic friction coefficient. The force  $F$  is contrary to the particle motion. The plus sign corresponds to the situation where the particle moves from the right to the left and the minus sign when it moves backward. From second Newton's law of motion, it is easy to find the position of the particle in time as  $X(t) = X(t_0) + V(t_0)t \pm \frac{1}{2}\alpha t^2$ , where  $X$  and  $\alpha = \mu g/(\omega^2 l)$  are the dimensionless position and acceleration of the particle, respectively. For  $\alpha = 0$  all results for the nondissipative case are obtained.

Using dimensionless variables, the motion of the particle is described by a two-dimensional map of the type

$$T: \begin{cases} V_{n+1} &= \sqrt{V_n^2 + 2\alpha(X_n + X_{n+1}) - 4\alpha} + 2\epsilon \\ t_{n+1} &= t_n + \frac{1}{\alpha}(V_n - \sqrt{V_n^2 - 4\alpha}), \end{cases} \quad (2)$$

where  $X_{n+1}$  is the position of particle, and hence of the moving wall, at the instant of collision  $(n+1)$ th.

Since we are looking at conditions to suppress or not FA, the natural observable to be characterized is the average velocity. It is shown in Fig. 1 the behavior of  $\bar{V} \times n$  for  $V_0 = 1$ ,  $\alpha = 9 \times 10^{-4}$ , and different values of  $\epsilon$ . The average velocity is obtained as  $\bar{V} = 1/(n+1) \sum_{i=0}^n V_i$ . A striking result that emerges from Fig. 1 is that FA might either be observed or not for  $\alpha \neq 0$ . The curves of  $\bar{V}$  depend on the control parameters and initial velocities. In Fig. 1(a) it is clear the depen-

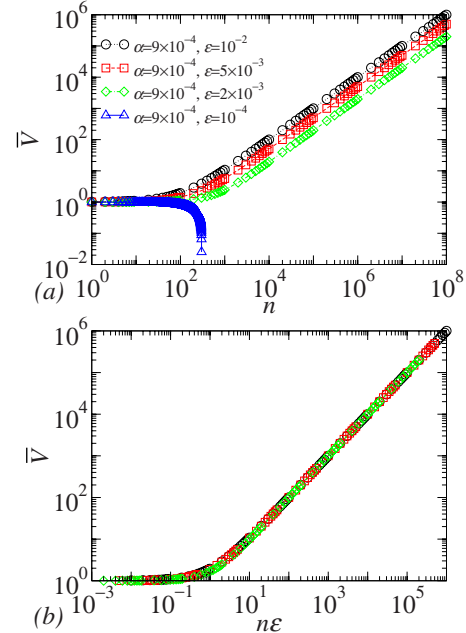


FIG. 1. (Color online) (a) Average velocity curves for  $V_0 = 1$ ,  $\alpha = 9 \times 10^{-4}$ , and different values of  $\epsilon$ , as labeled in the figure. (b) Collapse of some curves shown in (a) after a suitable rescale in the horizontal axis.

dence on the control parameter. The dependence on the initial velocity will be discussed latter. Basically, we observe that the average velocity stays almost constant for a long time and then it might rise or decrease. If the velocity decreases the particle reaches the rest. On the other hand, if FA is observed, after a characteristic changeover from a constant velocity to a regime of growth, the curve of  $\bar{V}$  grows with a law of the type  $\bar{V} \propto n$ . We see that different control parameters generate different curves. However, a rescaling in the horizontal axis is sufficient to merge all the curves onto a single curve, as it is shown in Fig. 1(b).

Let us discuss the dependence of the FA on the initial velocity. It is expected that there must exist some relation between the initial velocity,  $V_0$ , and parameters  $\epsilon$  and  $\alpha$ , which characterizes the transition from unlimited energy gain to completely energy dissipation. We now describe this transition.

The limit situation occurs when the amount of dissipated energy is exactly furnished to the particle by the moving wall. In this case the velocities after each collision satisfy the relation  $V_{n+1} = V_n = V_c$ . Because  $X_n \in [-\epsilon, \epsilon)$  we have that  $2\alpha(X_n + X_{n+1}) \in [-4\alpha\epsilon, 4\alpha\epsilon)$ . Therefore, regarding the velocity expression in map (2) and considering the extreme possibilities of  $2\alpha(X_n + X_{n+1})$ , we obtain the velocities  $V_-$  and  $V_+$

$$V_- = \frac{\epsilon^2 + \alpha(1 - \epsilon)}{\epsilon}, \quad V_+ = \frac{\epsilon^2 + \alpha(1 + \epsilon)}{\epsilon}. \quad (3)$$

In this sense we observe that for  $V_0 < V_-$  the energy furnished by the moving wall to the particle at each collision is smaller than the energy dissipated across the trajectory. Therefore after some time the particle losses all its energy, stopping between the two walls.

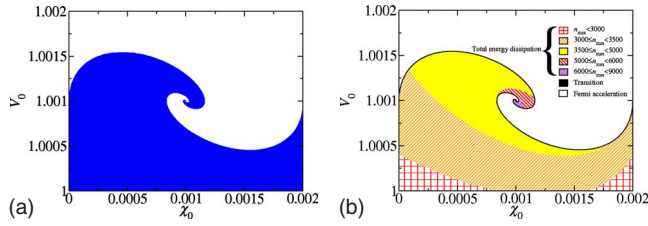


FIG. 2. (Color online) (a) Combinations of initial conditions for which the particle experiences FA, white region, and for which the particle loses energy until to reach the rest, blue (dark) region. (b) The white region corresponds to combinations of initial conditions that results in Fermi acceleration and the regions with different color (gray) patterns illustrate the maximum collision number before the total energy dissipation. The values of parameters are  $\varepsilon=10^{-3}$  and  $\alpha=10^{-3}$ .

On the other hand, for  $V_0 > V_+$  the amount of energy furnished by the wall at each collision with the particle is larger than the energy dissipated due to the friction between two impacts with the moving wall. Therefore, the system presents a net increase in particle's velocity after each collision, resulting in FA.

For the intermediate situation where the initial velocity of the particle lies in  $V_- < V_0 < V_+$ , the energy of the particle might grows without limits or not. Basically it depends on the combination of initial conditions  $\chi_0$  and  $V_0$ . Figure 2 allows us to understand the general behavior of the velocity curves for this situation. We used  $\varepsilon=10^{-3}$ ,  $\alpha=10^{-3}$ , and defined a grid of  $600 \times 600$  initial conditions with  $V_- < V_0 < V_+$  and  $0 \leq \chi_0 < 2\varepsilon$ . For each initial condition, map (2) was iterated and the asymptotic behavior of the trajectory of the particle was analyzed. If the velocity of the particle becomes greater than  $V_+$ , then the particle presents FA. If the velocity becomes smaller than  $V_-$  then the particle loses all its energy. In this way the white color in Fig. 2(a) corresponds to the initial conditions for which FA occurs. The blue (dark) color in Fig. 2(a) represents the initial conditions for which the iteration of map (2) results in total energy dissipation. Hence the particle stops between the walls after colliding against the moving wall  $n_{\max}$  times. The value of maximum collisions number  $n_{\max}$  depends on the initial conditions. The color (gray) patterns used in Fig. 2(b) illustrates the maximum collision number  $n_{\max}$  before the particle's kinetic energy is completely absorbed. The black line in Fig. 2(b) corresponds to the border that separates the suppression from the FA phenomena and corresponds to the numerical approximation of  $V_c$  for those parameters values.

We now discuss a scaling present for the average velocity as function of the control parameters and initial conditions, then leading to FA for the limit of  $V_0 \gg V_+$ . First it is important to understand the dependence of  $\bar{V}$  as a function of variable  $n$ , parameters  $\varepsilon$ ,  $\alpha$ , and initial velocity  $V_0$ . We initially kept fixed  $\varepsilon=10^{-3}$ ,  $V_0=10$  and performed some simulations of  $\bar{V} \times n$  for different values of  $\alpha$  as shown in Fig. 3(a). We note that different values of  $\alpha$  seem not to affect the  $\bar{V}$  curves. Therefore  $\alpha$  is not considered in the scaling analysis. Figure 3(b) shows four curves of  $\bar{V}$  for  $\alpha=10^{-5}$  and different values of  $\varepsilon$  and  $V_0$ . For small values of  $n$  we observe that  $\bar{V}$

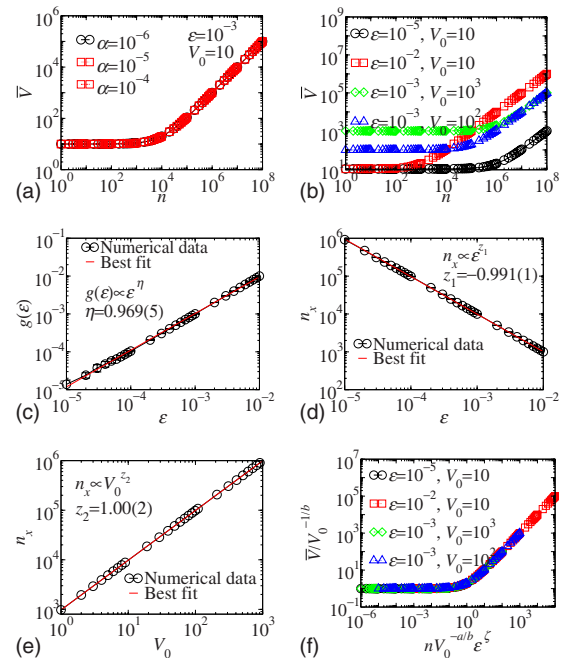


FIG. 3. (Color online) (a) Behavior of  $\bar{V} \times n$  for  $\varepsilon=10^{-3}$ ,  $V_0=10$ , and different values of  $\alpha$ , (b) behavior of  $\bar{V} \times n$  for  $\alpha=10^{-5}$  and different values of  $\varepsilon$  and  $V_0$ . (c) Log-log plot of  $g(\varepsilon)=\bar{V}/n^\beta$  as function of  $\varepsilon$ . (d) The best fit to the numerical data on the  $n_x$  versus  $\varepsilon$  plot furnishes  $z_1=-0.991(1)$ . (e) Log-log plot of  $n_x$  as function of  $V_0$ . (f) Collapse of  $\bar{V}$  curves of (b) onto a single and universal curve.

is constant and does not depend on  $\varepsilon$ . Moreover, in this initial plateau,  $\bar{V} \approx V_0$ . For large values of  $n$ ,  $\bar{V}$  depends on  $n$  and  $\varepsilon$  according to  $\bar{V} \propto n^\beta g(\varepsilon)$ , where  $\beta$  is the growth exponent and  $g$  is a function of  $\varepsilon$ . The changeover from the regime of constant value to the growth regime of  $\bar{V}$  is marked by a characteristic crossover  $n_x$  given by  $n_x \propto \varepsilon^{z_1} V_0^{z_2}$ , where  $z_1$  and  $z_2$  are dynamical exponents.

The exponent  $\beta$  is obtained via a nonlinear fit in the growth regime. The average value we obtained for 55  $\bar{V}$  curves with  $\varepsilon \in [10^{-5}, 10^{-2}]$  and  $V_0 \in [10^0, 9 \times 10^2]$  is  $\beta=0.9972(7)$ . Figure 3(c) shows a log-log plot of  $g(\varepsilon)=\bar{V}/n^\beta$  as function of  $\varepsilon$ . Performing power-law fittings to the numerical data we obtain  $g(\varepsilon) \propto \varepsilon^\eta$  with  $\eta=0.969(5)$ . In order to obtain the exponents  $z_1$  and  $z_2$  we performed two sets of simulations. Figure 3(d) shows the crossover  $n_x$  for different values of  $\varepsilon$  with fixed  $V_0=10$ . Applying power law fittings to the numerical data we obtain  $z_1=-0.991(1)$ . Similarly, we performed a set of simulations with fixed  $\varepsilon=10^{-3}$  and different values of  $V_0$ . Figure 3(e) displays the results. The best fit to the numerical data furnishes  $z_2=1.00(2)$ .

With the above hypotheses we suppose that  $\bar{V}$  obeys a homogeneous function of type  $\bar{V}(n\varepsilon^\zeta, V_0)=l\bar{V}(l^a n\varepsilon^\zeta, l^b V_0)$ , where  $l$  is a scaling factor and  $a$  and  $b$  are scaling exponents. We show that  $\zeta$  is related to the critical exponents  $\beta$ ,  $\eta$ , and  $z_1$ . Choosing  $l=V_0^{-1/b}$  we obtain  $\bar{V}(n\varepsilon^\zeta, V_0)=V_0^{-1/b} f(V_0^{-a/b} n\varepsilon^\zeta)$ . From this expression we find  $n_x \propto \varepsilon^{-\zeta} V_0^{a/b}$ . Hence  $z_1=-\zeta$  and  $z_2=a/b$ . Considering  $n \ll n_x$ , where  $\bar{V}$  is constant, we obtain

$b=-1$ . For  $n \gg n_x$  we have  $f=(V_0^{-a/b} n \varepsilon^\zeta)^\xi$ . Thus we find  $\xi=\beta$ ,  $a=-1/\beta$ , and  $\zeta=\eta/\beta$ . Therefore we have  $a=-1.0028(7)$  and  $\zeta=0.972(6)$ . Applying appropriate scaling transformations along the axis of Fig. 3(b) we show that all curves merge together onto a single and universal curve, as shown in Fig. 3(f). This result confirms that, for any combination of  $\varepsilon$  and  $V_0$  above the critical region where FA is suppressed shall experience basically the same general behavior.

Let us now discuss the situation where one of the walls exhibit stochastic motion. It is well known that FA is also observed for the nondissipative stochastic Fermi based systems [17,22,23]. Someone can ask about the presence or lack of FA when the frictional dissipation for the stochastic Fermi-Ulam model is considered. Thus instead of the wall to furnish an increment  $2\varepsilon$  in velocity at each collision [Eq. (2)], we regard the situation where the moving wall furnishes an increment  $2z$  to the velocity of the particle, where  $z$  assumes a random value in the interval  $[-\varepsilon, \varepsilon)$ . In this case the velocity of the particle after the collision  $(n+1)$ th is  $V_{n+1} = |\sqrt{V_n^2 + 2\alpha(X_n + X_{n+1}) - 4\alpha + 2z}|$  and the expression of  $t_{n+1}$  is the same as shown in Eq. (2). The absolute value bars in the velocity expression prevent the particle to leave the region between the walls.

Figure 4 shows the velocity after each collision as function of  $n$  for two initial conditions and for both sawtooth and stochastic motion for  $V_0$  greater than  $V_+$  (expression (3)). We considered  $\varepsilon=10^{-2}$  and  $\alpha=10^{-5}$ . When the wall moves according to the sawtooth expression the particle experiences FA, as discussed before. When the wall moves stochastically we observe for some intervals of  $n$  that the velocity decreases while it increases for other intervals of  $n$ . After  $n=i$  collisions with the moving wall the particle's velocity matches the condition  $V_i < V_{\min}$ , where  $V_{\min} = \sqrt{2\alpha(2 - X_n - X_{n+1})}$ . Then the particle stops between the walls and the time to the collision  $i+1$  diverges. For the stochastic case if the particle's velocity has a finite value, then the particle stops after some collisions.

Note that a similar discussion applies to the situation

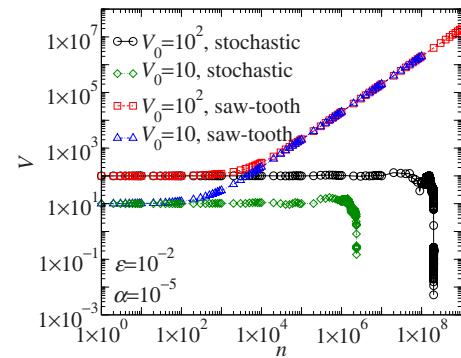


FIG. 4. (Color online) Velocity of the particle after each collision with the oscillating wall as function of  $n$  for the situation  $V_0 > V_+$ . The results were obtained for sawtooth and stochastic motion of the moving wall.

where the wall moves according to a sine function [15,24,25]. Similarly to the stochastic case, the velocity of the particle eventually becomes small and the particle loses all its energy.

As a final remark, we have considered a dissipative version of the one-dimensional Fermi accelerator model with sawtooth external perturbation in the presence of a dissipative force generated from a slip of a body against a rough surface. We showed that there exists a critical line that separates a region of total energy dissipation from a region where all initial conditions produce FA even in the presence of dissipation. Moreover, the behavior of the velocity curves is scaling invariant. Our results confirm that FA is sensible to the type of dissipation considered. In particular, a dissipation introduced via a friction force generated from a slip of a body against a rough surface is not a sufficient condition to suppress FA generically, but then it does happen under specific conditions.

D.G.L. thanks FAPEMIG and CNPq. E.D.L. thanks FAPESP, CNPq, and FUNDUNESP, Brazilian agencies.

- 
- [1] F. V. Hess, Phys. Z. **13**, 1084 (1912).  
[2] K. Greisen, Phys. Rev. Lett. **16**, 748 (1966).  
[3] T. G. Zatsépin and V. A. Kuzmin, Sov. Phys. JETP **4**, 78 (1966).  
[4] G. B. Gelmini, O. E. Kalashev, and D. F. Semikoz, J. Exp. Theor. Phys. **106**, 1061 (2008).  
[5] R. U. Abbasi *et al.*, Phys. Rev. Lett. **100**, 101101 (2008).  
[6] F. Fraschetti, Philos. Trans. R. Soc. London, Ser. A **366**, 4417 (2008).  
[7] E. Fermi, Phys. Rev. **75**, 1169 (1949).  
[8] S. S. Abdullaev and G. M. Zaslavsky, Phys. Plasmas **3**, 516 (1996).  
[9] A. Punjabi, H. Ali, and A. Boozer, Phys. Plasmas **4**, 337 (1997).  
[10] A. Iomin and Yu. Bliokh, Commun. Nonlinear Sci. Numer. Simul. **8**, 389 (2003).  
[11] E. D. Leonel, Phys. Rev. Lett. **98**, 114102 (2007).  
[12] G. A. Luna-Acosta, J. A. Méndez-Bermúdez, and F. M. Izrailev, Phys. Rev. E **64**, 036206 (2001); Phys. Lett. A **274**, 192 (2000).  
[13] G. A. Luna-Acosta, K. Na, L. E. Reichl, and A. Krokhin, Phys. Rev. E **53**, 3271 (1996).  
[14] E. D. Leonel, P. V. E. McClintock, and J. K. L. da Silva, Phys. Rev. Lett. **93**, 014101 (2004).  
[15] A. J. Lichtenberg and M. A. Leiberman, *Regular and Chaotic Dynamics* (Springer, New York, 1992).  
[16] R. Douady, Ph.D. thesis, Université Paris VII, 1982.  
[17] A. K. Karlis, P. K. Papachristou, F. K. Diakonou, V. Constantoudis, and P. Schmelcher, Phys. Rev. Lett. **97**, 194102 (2006); Phys. Rev. E **76**, 016214 (2007).  
[18] E. D. Leonel and A. L. P. Livorati, Physica A **387**, 1155 (2008).

- [19] Andre Luis Prando Livorati, D. G. Ladeira, and E. D. Leonel, Phys. Rev. E **78**, 056205 (2008).
- [20] E. D. Leonel, J. Phys. A: Math. Theor. **40**, F1077 (2007).
- [21] F. A. Souza, L. E. A. Simões, M. R. Silva, and E. D. Leonel, Math. Probl. Eng. **2009**, 409857 (2009).
- [22] J. M. Hammersley, *Proceedings of the Fourth Berkeley Symposium on Mathematical Statistics and Probability* (University of California Press, Berkeley, 1961), p. 79.
- [23] D. G. Ladeira and J. K. L. da Silva, J. Phys. A: Math. Theor. **40**, 11467 (2007).
- [24] E. D. Leonel, J. K. L. da Silva, and S. O. Kamphorst, Physica A **331**, 435 (2004).
- [25] J. K. L. da Silva, D. G. Ladeira, E. D. Leonel, P. V. E. McClintock, and S. O. Kamphorst, Braz. J. Phys. **36**, 700 (2006).